doi: 10.4149/gpb_2023024

Microbubbles activated by low-frequency ultrasound enhance the anti-tumor effects of curcumin in glioma cells by suppressing the TGF-β1/Smad/VEGF/NCAM signaling pathway

Lixia Mei[1,2], Zhen Zhang[1], Xiaole Song[1] and Xiaodi Zhao[1]

[1] *Department of Ultrasound, The First Affiliated Hospital of China Medical University, Shenyang City, Liaoning Province, China*
[2] *Department of Ultrasound, The First Hospital of Qiqihar city, Qiqihar city, Heilongjiang Province, China*

Abstract. This study investigated whether microbubbles activated by low-frequency ultrasound enhanced the anti-tumor effects of curcumin in glioma cells. CCK8 proliferation assay, scratch migration assay, and transwell invasion assay were performed to estimate the proliferation, migration, and invasion rates of the glioma cells in blank control and different treatment groups, respectively. Quantitative RT-PCR (qRT-PCR) analysis was performed to determine the relative expression levels of VEGF and NCAM mRNAs in the various experimental groups. Western blotting was performed to determine the activity status of the TGF-β1/Smad signaling pathway in various groups of glioma cells by estimating the expression levels of p-SMAD2/3, VEGF, and NCAM proteins. Combined treatment (Cur-Us-MBs) with microbubbles activated by low-frequency ultrasound and curcumin significantly reduced the in vitro proliferation, migration, and invasiveness of glioma cells compared to the control and other treatment groups. Furthermore, Cur-Us-MBs significantly reduced the expression levels of VEGF and NCAM mRNAs and proteins and p-Smad2/3 proteins , including those cells stimulated with rhTGF-β. These suggested that microbubbles activated by low-frequency ultrasound enhanced the inhibition of TGF-β1/Smad/VEGF/NCAM signaling pathway by curcumin, and enhanced the antitumor effects of curcumin by significantly reducing in vitro proliferation, migration, and invasiveness of glioma cells through this pathway.

Key words: Low-frequency ultrasound — Microbubbles — Curcumin — TGF-β1 — VEGF — NCAM

Introduction

Glioma is the most malignant and highly frequent primary tumor of the central nervous system. Gliomas are characterized by highly invasive, rapid, and diffuse growth. Furthermore, despite the availability of advanced treatments including surgery, radiotherapy, and chemotherapy, the survival outcomes of glioma patients are poor because of high tumor recurrence rates (Liu et al. 2018; Sun et al. 2019). Studies in animal models have shown that low-frequency ultrasound improves the efficacy of anti-tumor drugs by selectively inducing apoptosis of glioma cells (Zhang et al. 2012; Hsiao et al. 2013). Therefore, low-intensity ultrasound is a promising method for improving the efficacy of chemotherapeutic drugs in patients with glioma.

Currently, optimization of low-frequency ultrasound parameters is required to improve the clinical efficacy of anti-tumor therapy. Zhao et al. (2017) reported that low-intensity ultrasound (1 MHz and 12 MW power) treatment of locally irradiated rats with transplanted gliomas for 20 s significantly increased the permeability of the blood-brain

Correspondence to: Zhen Zhang, Department of Ultrasound, The First Affiliated Hospital of China Medical University, Shenyang City, Liaoning Province, 110001, China
E-mail: 2662898158@qq.com

barrier (BBB) and enhanced the delivery of diagnostic and chemotherapeutic drugs to the brain without significantly affecting the neuronal cells. Transforming growth factor-β (TGF-β) is a multifunctional cytokine that regulates cell growth, survival, and differentiation (Lawrence 1996). TGF-β also regulates epithelial-mesenchymal transition (EMT), tumor immune responses, tumor angiogenesis, and tumor metastasis (Meulmeester and Ten Dijke 2011; Connolly et al. 2012). TGF-β signaling promotes glioma cell proliferation and invasiveness (Wesolowska et al. 2011). But the specific mechanism by which it affects the biological activity of tumor cells remains unclear (Seoane et al. 2004).

Vascular endothelial growth factor (VEGF) is a central player in tumor angiogenesis, which is associated with tumor progression and metastasis (Yao and Zhang 2019). Tumor vascularization also plays a significant role in the progression of gliomas and other tumors *via* activation of the TGF-β1/Smad/PDGF (pro-platelet growth factor) signaling pathway. Neural cell adhesion molecule (NCAM) is a key protein in the intercellular junctions between neurons and glial cells and plays a key role in cellular recognition, tumor metastasis and growth, nerve regeneration, and transmembrane signaling (Zhang et al. 2011). Dysregulation of NCAM is implicated in several neurological diseases and tumors (Schmid et al. 2008). VEGF and NCAM factors are associated with tumor growth and metastasis, and play a key role in defining the biological characteristics of cancer cells.

A previous study by our group found that curcumin and ultrasound alone could inhibit the proliferative effect of glioma, and the combination of the two could achieve a better effect (Yao and Zhang 2019). The experiments showed that LFS (low-frequency ultrasound) can effectively open the BBB and ensure normal brain tissue is not damaged, while the opening of the BBB by LFS combined with microbubbles has a higher safety profile, and the cavitation effect of LFS combined with microbubbles greatly enhances the permeability of the cell membrane, and can also make the BBB endothelial cells inter gap widen, so that drugs can more easily enter the BBB. Because of the focused of ultrasound, the cavitation effect produced by the microbubbles was limited to the intravascular space, guaranteeing the controllability of the local opening of the BBB (Mei and Zhang 2021).

Recent studies have shown that microbubbles activated by low-frequency ultrasound enhance the anti-tumor effects of chemotherapeutic drugs (Luo et al. 2017; Zhang et al. 2018; Zhao et al. 2018). However, the mechanisms by which microbubbles activated by low-frequency ultrasound inhibit glioma growth and development are not clear. Therefore, in this study, we investigated whether microbubbles activated by low-frequency ultrasound enhance the anti-tumor effects of curcumin in glioma cells and the underlying mechanism of action.

Materials and Methods

Drugs and reagents

Curcumin was purchased from Sigma (UPN08511, Burlington, MA, USA). Sonazoid was purchased from GE Healthcare (ATC code: V08DA, Chicago, IL, USA). The rabbit anti-human VEGF antibody (Cat. No: ab36059) and rabbit anti-human NCAM antibody (Cat. No: ab30504) were purchased from Abcam (Cambridge, UK). Fetal bovine serum (FBS, F12350), DMEM (D17370), and trypsin (GCCC0136) were purchased from Hyclone Lab., QRT-PCR kit was purchased from (Cat. No: AG21017, Accurate biotechnology China).

Cell lines and cell culture

U251 and C6 glioma cells were purchased from the Shanghai Jikai Gene Chemical Technology Company (Shanghai, China) and cultured in DMEM medium containing 10% FBS in a humidified incubator maintained at 37°C and 5% CO_2.

Experimental glioma cell grouping

To determine if the microbubbles activated by low-frequency ultrasound enhanced the tumor suppressive effects of curcumin, glioma cells were divided into the following treatment groups: (1) Control: blank control group, no treatment; (2) Cur: treatment only with 15 μmol/l curcumin (Yao et al. 2019); (3) Cur-Us: treatment with 15 μmol/l curcumin after ultrasound irradiation administration with an intensity of 142.0 MW/cm^2 for 30 s (Zhang et al. 2013); (4) Us-MBs: incubation with 1–5×10^6/ml Sonazoid microbubbles (Li et al. 2016) followed by ultrasound irradiation for 30 s; (5) Cur-Us-MBs: incubation with Sonazoid microbubbles followed by treatment with 15 μmol/l curcumin, and subsequent ultrasound irradiation for 30 s.

To analyze if the Cur-Us-MBs inhibited glioma proliferation and progression through the TGF-β/SMAD signaling pathway, glioma cells were treated with recombinant human TGF-β1 (rh TGF-β1, Cat. No: 100-21, PEPROTCH, USA) or SMAD inhibitor (ITD-1, Cat. No: S6713, Selleck, USA). The following experimental groups of cells were studied: (1) Control: blank control group, no treatment; (2) rhTGF-β: administration of 10 ng/ml rhTGF-β (Li et al. 2019); (3) rhTGF-β1+Cur-Us-MBs: administration of 10 ng/ml rhTGF-β, followed by 1–5×10^6/ml microvesicles and 15 μmol/l curcumin, followed by ultrasound irradiation for 30 s; (4) Cur-Us-MBs: ultrasound irradiation was administered for 30 s after addition of microbubbles and curcumin; (5) Inhibitor ITD-1: cells were treated with 5 μmol/ml Smad2/Smad3 phosphorylation inhibitor (Willems et al. 2012). The cells in all the above groups were cultured for 24 h.

One vial of Sonazoid was reconstituted with 2 ml of normal saline and measured 1–5×10^6/ml. 6 well plates cells were added with 20 µl/ml, and 12 well plates were added with 10 µl/ml. Taking 6 well plates as an example, after glioma cells were adherent, Sonazoid was added, and the ultrasonic instrument was adjusted to ultrasonic frequency of 1 MHz, mechanical index of 1.5, and ultrasonic intensity of 142.0 MW/cm^2. The ultrasound probe was coated with coupling agent and tightly fitted to the bottom of 6 well plates and irradiated for 30 s. The mentioned dosage of curcumin and ultrasonic irradiation parameters were all previously standardized by our research group (Zhang et al. 2012; Yao et al. 2019).

CCK-8 proliferation assay

The glioma cells after treatments were seeded in 96 well plates (5000 cells/well in 100 µl medium), incubated in a humidified incubator at 37°C, and allowed to adhere. Then, the culture medium was aspirated out and replaced with 100 µl of culture medium containing 10% CCK-8 reagent (BS350B, biosharp, China). The cells were further incubated for 2 h at 37°C. Then, the absorbance was measured in a microplate reader at 450 nm.

Scratch assay for estimating migration rate of glioma cells

The U251 and C6 cells (5.0×10^5–1.0×10^6 *per* well) were seeded in 6-well plates and incubated in a humidified chamber at 37°C and 5% CO_2 for 24 h. After the cells adhered, a scratch mark was made perpendicular to the well plate with a 10 µl pipette tip. The cell culture medium was aspirated out. The plates were gently rinsed 2–3 times with PBS to remove cell debris. Then, fresh serum-free medium was added to all the wells. The samples were photographed and recorded at 0, 6, 12, and 24 h to determine the rate of migration into the scratch mark.

Transwell invasion assay

The upper chamber of the Transwell was coated with 80 µl of diluted Matrigel and allowed to dry in a humidified chamber at 37°C for 30 min. Then, 200 µl of cell suspension in culture medium without FBS (4.0×10^5 cells/well) was added in the upper chamber, and 600 µl of culture medium with 20% FBS was added to the lower chamber. Then, the Transwell chambers were incubated at 37°C and 5% CO_2 in a humified incubator (U251 cells were incubated for 24 h and C6 cells were incubated for 12 h).

After incubation, the upper chamber was removed. The liquid was slowly drained out by blotting. The cells on the upper surface of the membrane were removed. The cells on the lower side of the membrane (migrated cells) were fixed with 4% paraformaldehyde solution for 30 min at room temperature. The cells were air dried, stained with 0.1% crystal violet for 30 min, and observed under a light microscope. The number of cells on the lower surface of the membrane were counted in five different fields using an inverted microscope at a magnification of 200× and photographed.

Western blotting

Glioma cells were lysed in ice-cold RIPA buffer. The protein concentrations of the total cellular protein lysates were estimated using a BCA Kit (Cat. No: P0010S, Beyotime). Then, equal amounts of protein samples (15 µg *per* lane) were separated on 6% or 12% polyacrylamide gels using the mini protean III electrophoresis system (BioRad, Hercules, CA, USA). The separated proteins were transferred onto polyvinylidene fluoride (PVDF) membranes. The PVDF membranes were then blocked by incubation with 5% nonfat dry milk in a test buffer for 2 h, washed with TBST buffer, and incubated overnight with primary antibodies, namely, anti-VEGF (1:200), anti-NCAM (1:2000), and anti-GAPDH (1:5000) at 4°C. After washing three times with TBST, the membranes were incubated with the corresponding HRP-conjugated secondary antibodies for 2 h at room temperature. Finally, the specific protein bands were developed using the Enhanced chemiluminescent reagent (BioRad, USA). The protein bands were quantified using the ImageJ software.

Table 1. Primer sequences

Primer	Forward (5'-3')	Reverse (5'-3')
Human-NCAM	TTCATAGTCCTGTCCAACAACTACC	CCCTCACAGCGATAAGTGCC
Human-VEGF	CCTCTTGGAATTGGATTCGC	TGTATGTGGGTGGGTGTGTCTAC
Human-Smad2	CTTCTGTCATAGCATTGTGTGTG	GACCTCAAGTGCTGTTTTCTCTCTT
Human-Smad3	AAACACACGAGCAAACCCAGA	GTTCTGCTCACTTAAGCCACCA
Rat-NCAM	CTGGAACGCCGAGTACGAA	CGAAGTGAGCTGCCTTGGATT
Rat-VEGF	AAGAGGACAGAGAGACAGATGACAG	GGGTGCTCTTGCAGAATCTAGTG
Rat-Smad2	TGTCCAGTGGGTCTTAGCATTC	GGCACAAAGAGCCTGGAAGTT
Rat-Smad3	TGGAGCTGGAAGTGCGTGA	TGGGATGACCTCGTTGTTGAG

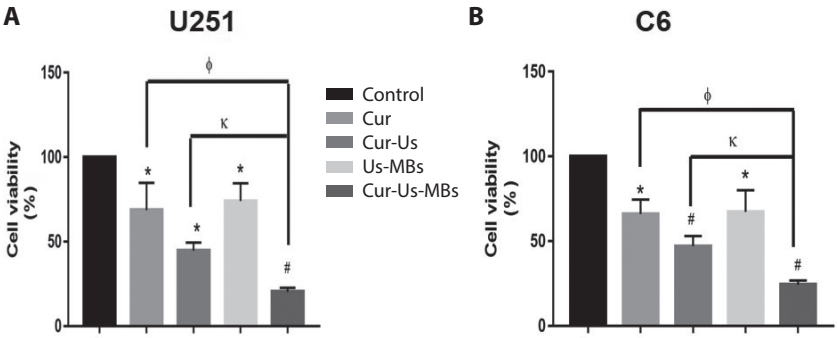

Figure 1. Combination treatment significantly reduces *in vitro* proliferation of U251 (**A**) and C6 (**B**) glioma cells. CCK-8 assay results show the proliferation rates of glioma cells in control and different treatment groups. The data are represented as means ± SD ($n = 3$). * $p < 0.05$ and # $p < 0.0001$ *vs.* control; $^{\Phi}$ $p < 0.05$ Cur *vs.* Cur-Us-MBs; ^{k} $p < 0.05$ Cur-Us-MBs *vs.*Cur-Us. **U251 cells** (Cur: F = 70.457, df = 1, $p = 0.006$; Us-MBs: F = 5.947, df = 1, $p = 0.05$; Cur-Us-MBs: F = 116.318, df = 1, $p = 0.000$). **C6 cells** (Cur: F = 5.979, df = 1, $p = 0.04$; Us-MBs: F = 7.524, df = 1, $p = 0.025$; Cur-Us-MBs: F = 145.101, df = 1, $p = 0.000$). Control, control group, no treatment; Cur, treatment with 15 μmol/l curcumin; Cur-Us, treatment with 15 μmol/l curcumin after ultrasound irradiation administration; Us-MB, incubation with $1–5\times10^6$/ml Sonazoid microbubbles followed by ultrasound irradiation for 30 s; Cur-Us-MBs, incubation with Sonazoid microbubbles followed by treatment with 15 μmol/l curcumin, and subsequent ultrasound irradiation for 30 s.

Real-time quantitative PCR (RT-qPCR)

Total RNA was extracted from the glioma cells using the Trizol reagent (Cat.No:15596026, Invitrogen, Grand Island, NY, USA) according to the manufacturer's instructions. RNA concentration of the samples was measured at 260 nm using the Biospec nanodrop (Shimadzu Corporation, MA, USA). Then, cDNA samples were prepared from equal amounts of RNA using the PrimeScriptRT Reagent Kit with the gDNA Eraser (Cat.No: AG21017, Accurate biotechnology China). The RT-qPCR primers are listed in Table 1.

RT-qPCR amplification was performed with a 20-μl reaction mixture containing 0.5 μmol/l of forward and reverse primers, 0.2 μg cDNA as template, (GAPDH primers as internal reference), and SYBR green qPCR mix reagents. The RT-qPCR protocol included 45 cycles with pre-denaturation at 95°C for 30 s, PCR amplification at 95°C for 5 s, 60°C for 30 s, melting at 95°C for 5 s, extension at 60°C for 1 min, and cooling at 40°C for 30 s. The relative mRNA expression was determined using the $2^{-\Delta\Delta Ct}$ method.

Statistical analysis

Statistical analysis was performed using the SPSS statistical software version 21.0 (SPSS, Chicago, IL, USA) and GraphPad prism software (GraphPad Software, Inc., La Jolla, CA, USA). The data were expressed as mean ± standard deviation (SD). The data was analyzed by two-way analysis of variance (ANOVA) followed by Bonferroni *post hoc* tests. $p < 0.05$ was considered statistically significant. All the experiments were repeated at least three times.

Results

Enhancement of glioma inhibition by curcumin using ultrasound combined with microbubbles: Cur-Us-MBs significantly reduces in vitro proliferation of glioma cells

CCK-8 assay results demonstrated that the proliferation of glioma cells was significantly inhibited in all the treatment groups, especially the Cur-Us-MBs group compared with the Control group ($p < 0.05$ or $p < 0.0001$; Fig. 1). Furthermore, the proliferation rates of glioma cells were significantly lower in the Cur-Us-MBs group compared to the glioma cells in the Cur group and the Cur-Us group ($p < 0.05$ for both; Fig. 1).

Treated groups influence migration of glioma cells

Scratch assay was performed to analyze the *in vitro* migration rates of glioma cells at 0, 6, 12, and 24 h. The results showed that compared with the control cells, the migration ability of cells in all the treatment groups were reduced at 12 h, and the differences were more significant at 24 h ($p < 0.05$, $p < 0.0001$). The migration rates of glioma cells in the Cur-Us-MBs group were significantly lower than those in the Cur group and Cur-Us group (Fig. 2).

Treated groups reduces invasiveness of glioma cells

Transwell invasion assay results showed that except for the Us-MBs group of the C6 cell line, the invasiveness of the glioma cells in all the other treatment groups were lower than the glioma cells in the Control group (Fig. 3). Furthermore, the invasiveness of glioma cells in the Cur-Us-MBs group

were significantly lower compared with the glioma cells from the other treatment groups ($p < 0.05$; Fig. 3).

Cur-Us-MBs down-regulated expressions of VEGF and NCAM protein levels

Western blot analysis showed that VEGF and NCAM protein expression levels were significantly reduced in all the treatment groups compared to the Control group (Fig. 4). Furthermore, expression levels of VEGF and NCAM proteins in the Cur-Us-MBs group were significantly lower than those in the Cur group and the Cur-Us group ($p < 0.05$; Fig. 4).

Cur-Us-MBs down-regulates the expressions of VEGF and NCAM at mRNA level

QRT-PCR results showed that except for VEGF mRNA levels in the U251 Us-MBs group and NCAM mRNA levels in the C6 Us-MBs group, VEGF and NCAM mRNA expression levels were significantly lower in all the other treatment groups (Fig. 5). Furthermore, VEGF and NCAM mRNA levels in the Cur-Us-MBs group were significantly lower than those in the Cur group and the Cur-Us group ($p < 0.05$; Fig. 5). This suggested that Cur-Us-MBs inhibited TGF-β1/Smad signaling pathway in the glioma cells.

The Cur-Us-MBs in vitro may affect TGF-β1/Smad signaling pathway to achieve inhibition: Cur-Us-MBs reduces VEGF and NCAM protein levels in the glioma cells

We analyzed the effects of Cur-Us-MBs on the TGF-β1 signaling pathway in the glioma cells. Western blot analysis showed that treatment of glioma cells with rhTGF-β significantly increased the expression levels of phosphorylated Smad2/3 (p-Smad2/3) and the expression levels of VEGF and NCAM proteins in both U251 or C6 glioma cells ($p < 0.05$). In contrast, VEGF and NCAM protein levels were signifi-

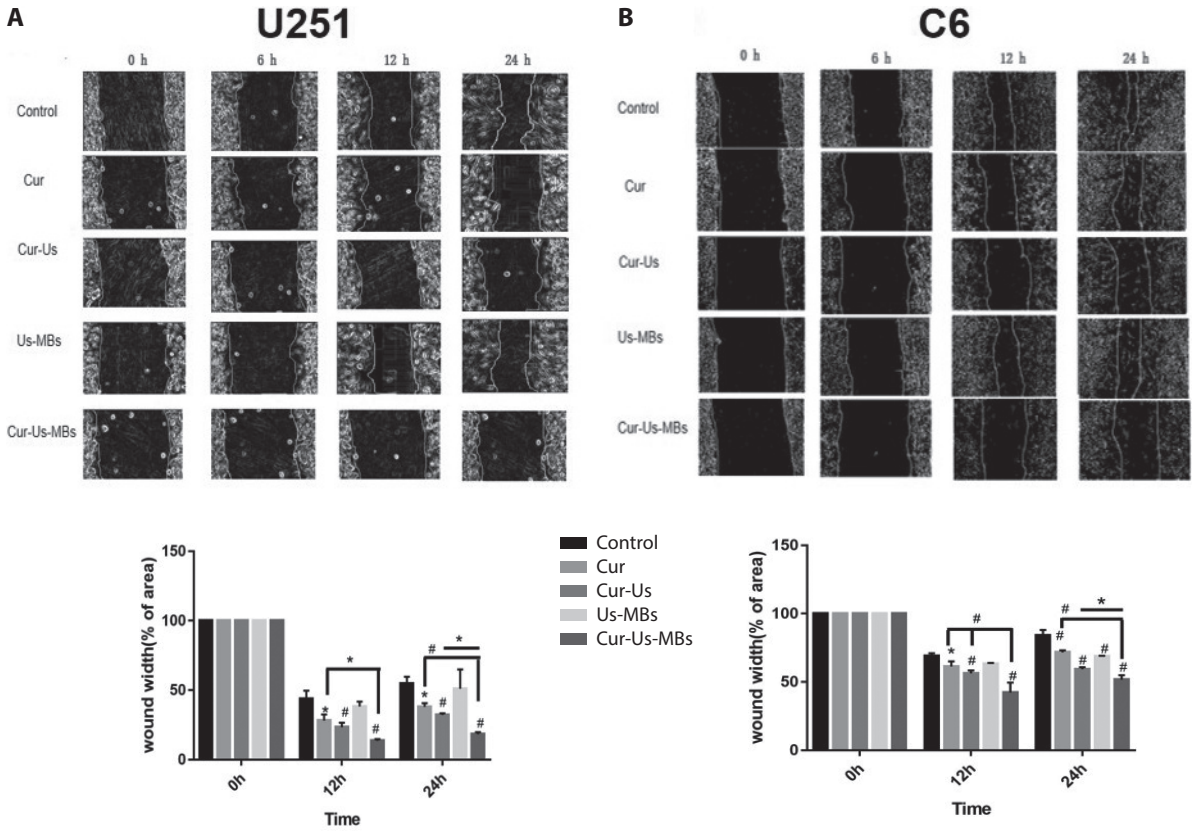

Figure 2. Combination treatment significantly reduces *in vitro* migration of U251 (**A**) and C6 (**B**) glioma cells. Representative images (4×10 magnification) show the results of the scratch migration assay in control and different treatment groups of glioma cells at 0, 6, 12, and 24 h. Quantitative analysis (below images) shows the migration rates of the glioma cells in the Control, Cur, Cur-Us, Us-MBs, and Cur-Us-MBs groups at 0, 12, and 24 h. The data are represented as means ± S.D ($n = 3$). * $p < 0.05$, # $p < 0.0001$. **U251 cells** (Cur: F = 73.096, df = 1, $p = 0.000$; Us-MBs: F = 136.651, df = 1, $p = 0.000$; Cur-Us-MBs: F = 59.452, df = 1, $p = 0.000$). **C6 cells** (Cur: F = 120.432, df = 1, $p = 0.000$; Us-MBs: F = 105.394, df = 1, $p = 0.000$; Cur-Us-MBs: F = 45.240, df = 1, $p = 0.000$). For abbreviations, see Figure 1.

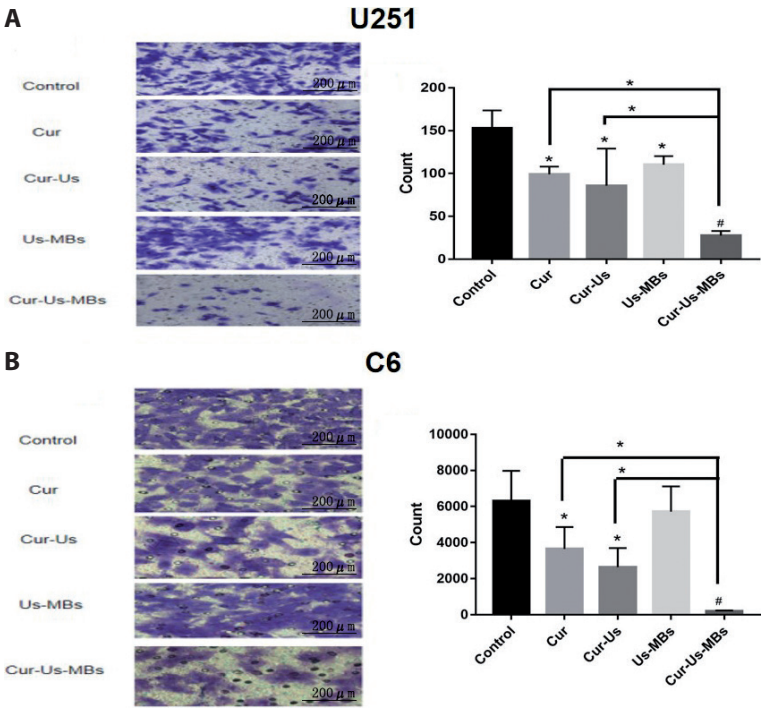

Figure 3. Combination significantly reduces *in vitro* Transwell invasion of U251 (**A**) and C6 (**B**) glioma cells. Representative images (×200 magnification) show the Transwell invasion of glioma cells in control and different treatment groups. Quantitative analysis shows the number of invasive glioma cells. The data are represented as means ± SD ($n = 3$). * $p < 0.05$, # $p < 0.0001$. **U251 cells** (Cur: F = 68.312, df = 1, $p^- = 0.000$; Us-MBs: F = 65.984, df = 1, $p^- = 0.000$; Cur-Us-MBs: F = 5.950, df = 1, $p^- = 0.041$). **C6 cells** (Cur: F = 55.473, df = 1, $p^- = 0.000$; Us-MBs: F = 14.560, df = 1, $p^- = 0.005$; Cur-Us-MBs: F = 6.967, df = 1, $p^- = 0.030$). For abbreviations, see Figure 1.

cantly reduced in the glioma cells treated with the Smad2/3 inhibitor ITD-1 and were comparable with the VEGF and NCAM protein levels in the Cur-Us-MBs group ($p > 0.05$). Furthermore, compared with control, glioma cells in the Cur-Us-MBs plus rhTGF-β group did not show upregulation of phosphorylated Smad2/3 (p-Smad2/3) levels or VEGF and NCAM protein levels ($p > 0.05$; Fig. 6).

Cur⁻Us⁻MBs reduces VEGF and NCAM at mRNA levels in the glioma cells

QRT-PCR analysis showed that activation of the TGF-β1/Smad signaling pathway by rhTGF-β significantly increased the expression levels of VEGF and NCAM mRNAs in the glioma cells. In contrast, inhibition of Smad2/3 by ITD-1 decreased the expression levels of VEGF and NCAM mRNAs, which were comparable to the expression levels in the Cur-Us-MBs group ($p > 0.05$). In the glioma cells belonging to the Cur-Us-MBs group that were also treated with rhTGF-β, VEGF and NCAM mRNA levels were comparable with the control group ($p > 0.05$; Fig. 7).

Discussion

Tumorigenesis is a complex multi-step process involving genetic and epigenetic mechanisms that result in activation of multiple oncogenes and inactivation of several tumor suppressor genes (Bergers and Benjamin 2003). In brain tumors, survival rates are low because of poor drug penetration due to the BBB. This prevents uptake of optimal concentrations of chemotherapeutic drugs into the brain tumors and increases the resistance of tumors against chemotherapeutic drugs. Therefore, improved penetration of chemotherapeutic drugs through the BBB is required to reduce the intake of larger doses of chemotherapeutic drugs, which are responsible for increased systemic cytotoxicity and drug resistance in glioma patients. In this study, we investigated whether microbubbles activated by low-frequency ultrasound would enhance the anti-tumor effects of curcumin in the glioma cells and the underlying mechanism.

Previous studies have demonstrated that microbubbles active by low-frequency ultrasound improved targeted drug delivery to the brain tumor tissues by increasing the permeability of the BBB (Qian et al. 2018; Wang et al. 2019). Focused ultrasound and SonoVue® SF6-coated ultrasound microbubbles increased chemotherapeutic drug concentrations in the tumors by more than two-fold in rats with orthotopically grafted gliomas and also enhanced the median survival time compared to the corresponding control rats (Wei et al. 2013; Aryal et al. 2015). Sonazoid is another microbubble that is made of phospholipid-encapsulated perfluorobutane with a diameter of 1.0–5.0 μm. The concentration of Sonazoid microvesicles is approximately $2.0–5.0\times10^8$/ml. Compared with conventional SonoVue, microvesicles are smaller in diameter and more

numerous *per* ml (SonoVue: microvesicles diameter 1.0–10.0 μm, 2.0~2.5×10/ml). It is more readily retained within capillaries, which prolongs its duration of action. Previous studies have shown that the diagnostic value and safety of Sonazoid and SonoVue are comparable. Peripheral intravenous injections of Sonazoid in a mouse model of cirrhosis showed normal vital signs including blood oxygen levels and electrocardiogram readouts and did not show any adverse effects based on routine blood and urine biochemistry (He et al. 2021). In this study, Sonazoid was chosen as the microbubble because of superior physical characteristics. The concentration of Sonazoid microbubbles was 1–5×10^6/ml (Qian et al. 2013).

Curcumin is an antitumor drug that strongly inhibits proliferation, migration, and invasion and induces apoptosis in several types of tumor cells (Alhasawi et al. 2022; Gao et al. 2022; Mekkawy et al. 2022; Zhu et al. 2022). In our previous study, 15 μmol/l curcumin significantly inhibited growth and proliferation of glioma cells (Yao et al. 2011). Therefore, in this study, we used a lower concentration of curcumin was chosen to minimize off-target effects.

VEGF and NCAM promote tumor cell proliferation, migration, and invasion, and play a key role in modulating the biological characteristics of tumors (Knowles et al. 2013). TGF-β1/Smad signaling pathway is activated in glioma tissues and promotes invasiveness of glioma cells

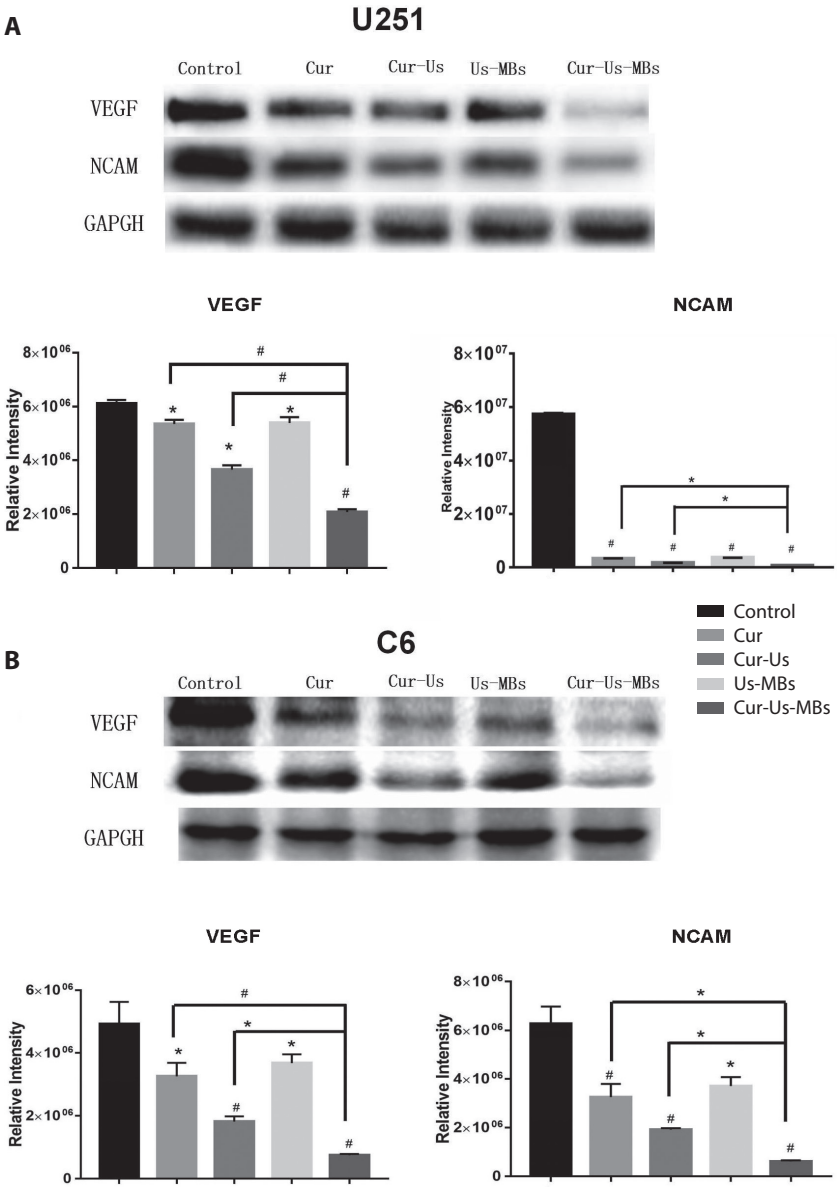

Figure 4. Combination treatment significantly reduces VEGF and NCAM protein expression levels in the U251 (**A**) and C6 (**B**) glioma cells. Histogram plots show the expression levels of VEGF and NCAM proteins in the glioma cells in control and different treatment groups. The data are represented as mean ± SD ($n = 3$). * $p < 0.05$, # $p < 0.0001$. **U251 cells: VEGF** (Cur: F = 322.198, df = 1, $p^- = 0.000$; Us-MBs: F = 313.542, df = 1, $p^- = 0.000$; Cur-Us-MBs: F = 126.709, df = 1, $p^- = 0.000$); **NCAM** (Cur: F = 17348.600, df = 1, $p^- = 0.000$; Us-MBs: F = 16898.272, df = 1, $p^- = 0.000$; Cur-Us-MBs: F = 13847.681, df = 1, $p^- = 0.000$). **C6 cells: VEGF** (Cur: F = 40.689, df = 1, $p^- = 0.003$; Us-MBs: F = 27.976, df = 1, $p^- = 0.006$; Cur-Us-MBs: F = 5.109, df = 1, $p^- = 0.048$); **NCAM** (Cur: F = 150.381, df = 1, $p^- = 0.000$; Us-MBs: F = 140.082, df = 1, $p^- = 0.000$; Cur-Us-MBs: F = 7.209, df = 1, $p^- = 0.043$). For abbreviations, see Figure 1.

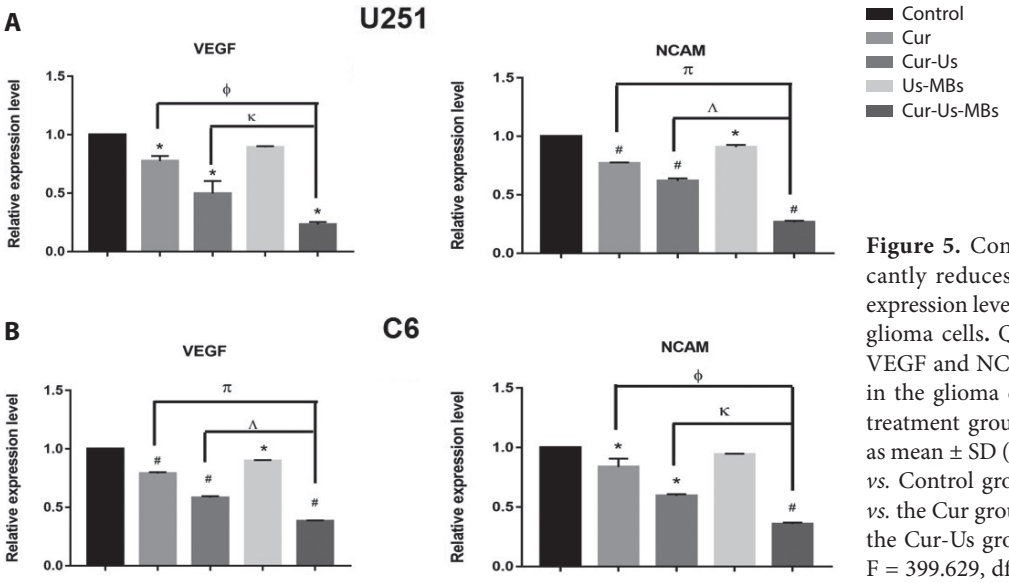

Figure 5. Combination treatment significantly reduces VEGF and NCAM mRNA expression levels in the U251 (**A**) and C6 (**B**) glioma cells**.** QRT-PCR analysis shows the VEGF and NCAM mRNA expression levels in the glioma cells in control and different treatment groups. The data are represented as mean ± SD ($n = 3$). * $p < 0.05$, $^{\#}$ $p < 0.0001$ *vs.* Control group; $^{\Phi}$ $p < 0.05$, $^{\pi}$ $p < 0.0001$ *vs.* the Cur group; $^{\kappa}$ $p < 0.05$, $^{\Lambda}$ $p < 0.0001$ *vs.* the Cur-Us group. **U251 cells: VEGF** (Cur: F = 399.629, df = 1, $p^{-} = 0.000$; Us-MBs: F = 226.633, df = 1, $p^{-} = 0.000$; Cur-Us-MBs: F = 103.834, df = 1, $p^{-} = 0.001$); **NCAM** (Cur: F = 2696.001, df = 1, $p^{-} = 0.000$; Us-MBs: F = 1256.888, df = 1, $p^{-} = 0.000$; Cur-Us-MBs: F = 601.680, df = 1, $p^{-} = 0.000$). **C6 cells: VEGF** (Cur: F = 4073.115, df = 1, $p^{-} = 0.000$; Us-MBs: F = 1997.833, df = 1, $p^{-} = 0.000$; Cur-Us-MBs: F = 719.423, df = 1, $p = 0.000$); **NCAM** (Cur: F = 221.138, df = 1, $p^{-} = 0.000$; Us-MBs: F = 115.222, df = 1, $p^{-} = 0.000$; Cur-Us-MBs: F = 70.558, df = 1, $p^{-} = 0.001$). For abbreviations, see Figure 1.

(Wesolowska et al. 2008). In this study, we investigated the effects of microbubbles activated by ultrasound on the anti-tumor effects of curcumin and the activity status of the TGF-β1/Smad signaling pathway in glioma cells. Our results showed that ultrasound combined with microbubbles enhanced the tumor suppressive effects of curcumin. The *in vitro* proliferation, migration, and invasiveness of glioma cells in the combination treatment group were significantly lower than in the other treatment and control groups. The glioma cells in the curcumin alone and ultrasound + curcumin groups also showed significantly lower proliferation, migration, and invasiveness than the untreated glioma cells. Furthermore, ultrasonic irradiation alone significantly improved the tumor suppressive effects of curcumin and was close to the effects of the combination treatment group. Western blotting and RT-qPCR experiments showed that VEGF and NCAM protein and mRNA expression levels were significantly lower in the combination treatment group compared to the other treatment and control groups.

We analyzed the status of the TGF-β1/Smad signaling pathway to determine the mechanisms underlying the anti-tumor effects of various treatments including the combination treatment in the glioma cells. By Western blot and RT-qPCR experiments, we found glioma cells in the rhTGF-β group showed significantly higher phosphorylated Smad2/Smad3 proteins and subsequent upregulation of VEGF and NCAM protein and mRNA expression levels. In contrast, inhibition of Smad2/Smad3 phosphorylation significantly decreased the expression levels of VEGF and NCAM mRNAs and proteins, and levels were similar to the levels in the Cur-Us-MBs treatment group. Furthermore, in the rhTGF-β+Cur-Us-MBs treatment group, the phosphorylated Smad2/Smad3 protein levels and the VEGF and NCAM protein and mRNA expression levels were similar to the control group. This conclusion proves that VEGF, NCAM, proposed by Knowles et al. (2013) is a critical factor for tumor cell proliferation, migration, and invasion. The experimental results are also in accordance with Wesolowska et al. (2008) who indicated that TGF-β1/Smad may be a key pathway in glioma cell proliferation and invasion. In our experimental grouping, the inhibition of glioma cells in Cur-Us group is consistent with the previous results of our working team (Yao et al. 2019). While in the Cur-Us-MBs group, we added microvesicle agents, the inhibition effect of which was better than the Cur-Us group. Confirmed the conclusion that ultrasound excited microbubbles open the tissue barriers, widen the intercellular space, increase the drug concentration in the tumor region, increase the inhibitory effect, proposed by Wei et al. (2013).

Our study has several drawbacks. First, several parameters such as ultrasonic sound intensity, microbubble diameter, and curcumin concentration were based on previous reports and were not optimized for our experiments. Second, it was not clear whether ultrasound + microbubble treatment inhibited the proliferation of glioma

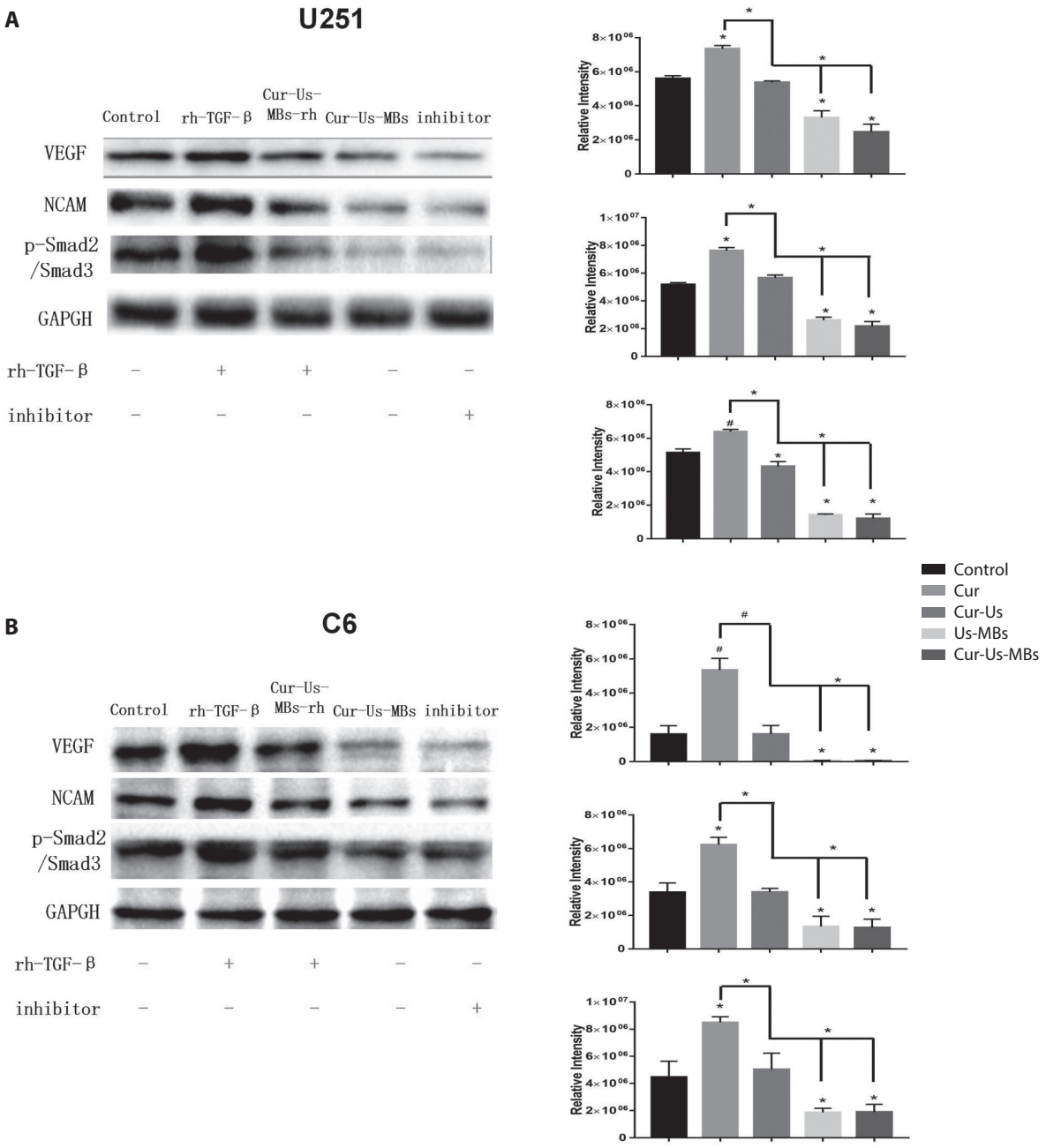

Figure 6. Combination treatment inhibits phosphorylation of Smad2/3 proteins and reduces the expression levels of VEGF and NCAM proteins in the U251 **(A)** and C6 (**B**) glioma cells. Histogram plots show the levels of p-Smad2/3, VEGF, and NCAM proteins in the glioma cells in control and different treatment groups. The data are represented as mean ± SD ($n = 3$). * $p < 0.05$, # $p < 0.0001$. **U251 cells: VEGF** (rh-TGF-β: F = 36.442, df = 1, $p^- = 0.004$; Cur-Us-MBs: F = 76.104, df = 1, $p^- = 0.001$. r-Us-MBs-rh-TGF-β: F = 0.112, df = 1, $p^- = 0.755$); **NCAM** (rh-TGF-β: F = 406.696, df = 1, $p^- = 0.000$; Cur-Us-MBs: F = 275.957, df = 1, $p^- = 0.000$. Cur-Us-MBs-rh-TGF-β: F = 4.774, df = 1, $p^- = 0.094$); **P-Smad2/Smad3** (rh-TGF-β: F = 218.288, df = 1, $p^- = 0.000$; Cur-Us-MBs: F = 424.530, df = 1, $p^- = 0.000$. Cur-Us-MBs-rh-TGF-β: F = 34.351, df = 1, $p^- = 0.004$). **C6 cells: VEGF** (rh-TGF-β: F = 87.250, df = 1, $p^- = 0.000$; Cur-Us-MBs: F = 86.881, df = 1, $p^- = 0.000$. Cur-Us-MBs-rh-TGF-β: F = 15.206, df = 1, $p^- = 0.005$); **NCAM** (rh-TGF-β: F = 78.782, df = 1, $p^- = 0.000$; Cur-Us-MBs: F = 77.778, df = 1, $p^- = 0.000$. Cur-Us-MBs-rh-TGF-β: F = 2.003, df = 1, $p^- = 0.195$); **P-Smad2/Smad3** (rh-TGF-β: F = 50.987, df = 1, $p^- = 0.000$; Cur-Us-MBs: F = 36.160, df = 1, $p^- = 0.000$. Cur-Us-MBs-rh-TGF-β: F = 0.718, df = 1, $p^- = 0.421$). Control, blank control group; rhTGF-β, administration of 10 ng/ml rhTGF-β; rhTGF-β1+Cur-Us-MBs, administration of 10 ng/ml rhTGF-β, followed by 1–5×10^6/ml microvesicles and 15 μmol/l curcumin, followed by ultrasound irradiation for 30 s; Cur-Us-MBs, ultrasound irradiation was administered for 30 s after addition of microbubbles and curcumin; Inhibitor, cells were treated with 5 μmol/ml Smad2/Smad3 phosphorylation inhibitor. For abbreviations, see Figure 1.

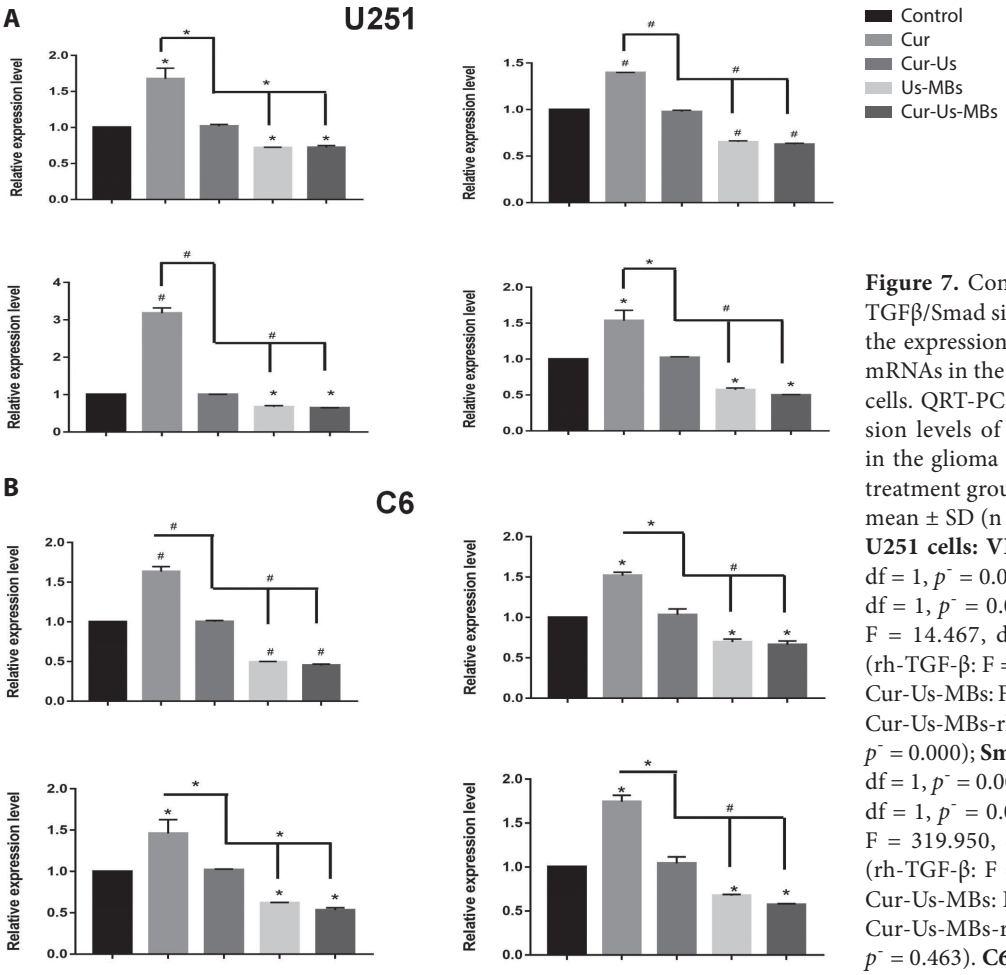

Figure 7. Combination treatment inhibits TGFβ/Smad signaling pathway and reduces the expression levels of VEGF and NCAM mRNAs in the U251 **(A)** and C6 (**B**) glioma cells. QRT-PCR analysis shows the expression levels of VEGF and NCAM mRNAs in the glioma cells in control and different treatment groups. The data are presented as mean ± SD (n = 3). * $p < 0.05$, # $p < 0.0001$. **U251 cells: VEGF** (rh-TGF-β: F = 86.674, df = 1, $p^- = 0.001$; Cur-Us-MBs: F = 76.104, df = 1, $p^- = 0.001$. Cur-Us-MBs-rh-TGF-β: F = 14.467, df = 1, $p^- = 0.023$); **NCAM** (rh-TGF-β: F = 1255.633, df = 1, $p^- = 0.000$; Cur-Us-MBs: F = 9473.573, df = 1, $p^- = 0.000$. Cur-Us-MBs-rh-TGF-β: F = 1255.633, df = 1, $p^- = 0.000$); **Smad2** (rh-TGF-β: F = 591.197, df = 1, $p^- = 0.000$; Cur-Us-MBs: F = 589.461 df = 1, $p^- = 0.000$. Cur-Us-MBs-rh-TGF-β: F = 319.950, df = 1, $p^- = 0.000$); **Smad3** (rh-TGF-β: F = 90.026, df = 1, $p^- = 0.001$; Cur-Us-MBs: F = 81.250, df = 1, $p^- = 0.001$. Cur-Us-MBs-rh-TGF-β: F = 0.656, df = 1, $p^- = 0.463$). **C6 cells: VEGF** (rh-TGF-β: F = 629.014, df = 1, $p^- = 0.000$; Cur-Us-MBs: F = 625.198, df = 1, $p^- = 0.000$. Cur-Us-MBs-rh-TGF-β: F = 7.487, df = 1, $p^- = 0.052$); **NCAM** (rh-TGF-β: F = 303.304, df = 1, $p^- = 0.000$; Cur-Us-MBs: F = 267.814, df = 1, $p^- = 0.000$. Cur-Us-MBs-rh-TGF-β: F = 1.159, df = 1, $p^- = 0.342$); **Smad2** (rh-TGF-β: F = 53.483, df = 1, $p^- = 0.002$; Cur-Us-MBs: F = 48.850, df = 1, $p^- = 0.002$. Cur-Us-MBs-rh-TGF-β: F = 0.282, df = 1, $p^- = 0.623$); **Smad3** (rh-TGF-β: F = 216.308, df = 1, $p^- = 0.000$; Cur-Us-MBs: F = 185.574, df = 1, $p^- = 0.000$. Cur-Us-MBs-rh-TGF-β: F = 24.713, df = 1, $p^- = 0.008$). For abbreviations, see Figure 6.

cells compared to the control group because the results for the scratch assay, Transwell invasion assay, and qRT-PCR assays varied between repeats. Therefore, the tumor suppressive effects of the Us-MBs group require further verification.

In summary, our results demonstrated that microbubbles activated by low-frequency ultrasound enhanced the tumor suppressive effects of curcumin in the glioma cells by inhibiting the TGF-β1/Smad/VEGF/NCAM signaling pathway. Therefore, TGF-β1/Smad signaling pathway is a potential therapeutic target for patients with gliomas. Furthermore, our study demonstrated that microbubbles activated by low-frequency ultrasound enhance the anti-tumor effects of curcumin *in vitro*, but the clinical significance of these findings requires further investigations.

Conflict of interest. The authors claim no conflicts of interest.

References

Alhasawi MAI, Aatif M, Muteeb G, Alam MW, Oirdi ME, Farhan M (2022): Curcumin and its derivatives induce apoptosis in human cancer cells by mobilizing and redox cycling genomic copper ions. Molecules **27,** 7410-7418 https://doi.org/10.3390/molecules27217410

AryalM Park J, Vykhodtseva N, Zhang YZ, McDannold N (2015): Enhancement in blood-tumor barrier permeability and delivery of liposomal doxorubicin using focused ultrasound and microbubbles: evaluation during tumor progression in a rat glioma model. Phys. Med. Biol. **60,** 2511-2527 https://doi.org/10.1088/0031-9155/60/6/2511

Bergers G, Benjamin LE (2003): Tumorigenesis and the angiogenic switch. Nature reviews. Cancer **3,** 401-410 https://doi.org/10.1038/nrc1093

Connolly EC, Freimuth J, Akhurst RJ (2012): Complexities of TGF-β targeted cancer therapy. Review Int. J. Biol. Sci. **8,** 964-978 https://doi.org/10.7150/ijbs.4564

Gao C, Zhang L, Xu M, LuoY, Wang B, Kuang M, LiuX Sun, M, Guo Y, Teng L, Wang C, Zhang Y, Xie J (2022): Pulmonary delivery of liposomes co-loaded with SN38 prodrug and curcumin for the treatment of lung cancer. Eur. J. Pharm. Biopharm. **179,** 156-165 https://doi.org/10.1016/j.ejpb.2022.08.021

He M, Zhu L, Huang M, Zhong L, Ye Z, Jiang T (2021): Comparison between sonovue and sonazoid contrast-enhanced ultrasound in characterization of focal nodular hyperplasia smaller than 3 cm. J. Ultrasound. Med. **40,** 2095-2104 https://doi.org/10.1002/jum.15589

Hsiao YS, Kumon RE, Deng CX (2013): Characterization of lesion formation and bubble activities during high intensity focused ultrasound ablation using temperature-derived parameters. Infrared Phys. Technol. **60,** 108-117 https://doi.org/10.1016/j.infrared.2013.04.002

Knowles LM, Gurski LA, Engel C, Gnarra JR, Maranchie JK, Pilch J (2013): Integrin αvβ3 and fibronectin upregulate Slug in cancer cells to promote clot invasion and metastasis. Cancer Res. **73,** 6175-6184 https://doi.org/10.1158/0008-5472.CAN-13-0602

Lawrence DA (1996): Transforming growth factor-beta: a general review. Eur. Cytokine Netw. **7,** 363-374

Li RD, Deng ZL, Hu N, Liang X, Liu B, Luo J, Chen L, Yin L, Luo X, Shui W, et al. (2012): Biphasic effects of TGFβ1 on BMP9-induced osteogenic differentiation of mesenchymal stem cells. BMB Reports **45,** 509-514 https://doi.org/10.5483/BMBRep.2012.45.9.053

Li Y, Wang P, Chen X, Hu J, Liu Y, Wang X, Liu Q (2016): Activation of microbubbles by low-intensity pulsed ultrasound enhances the cytotoxicity of curcumin involving apoptosis induction and cell motility inhibition in human breast cancer MDA-MB-231 cells. Ultrason. Sonochem. **33,** 26-36 https://doi.org/10.1016/j.ultsonch.2016.04.012

Liu H, Li C, Yang J, Sun Y, Zhang S, Yang J, Yang L, Wang Y, Jiao B (2018): Long noncoding RNA CASC9/miR-519d/STAT3 positive feedback loop facilitate the glioma tumourigenesis. J. Cell Mol. Med. **22,** 6338-6344 https://doi.org/10.1111/jcmm.13932

Luo W, Wen G, Yang L, Tang J, Wang J, Wang J, Zhang S, Zhang L, Ma F, Xiao L, Wang Y (2017): Dual-targeted and pH-sensitive doxorubicin prodrug-microbubble complex with ultrasound for tumor treatment. Theranostics **7,** 452-465 https://doi.org/10.7150/thno.16677

Mekkawy SA, Abdalla MS, Omran MM, Hassan NM, Abdelfattah R, Abdel-Salam IM (2022): Cancer stem cells as a prognostic biomarker and therapeutic target using curcumin/piperine extract for multiple myeloma. Asian Pac. J. Cancer Prev. **23,** 3507-3515 https://doi.org/10.31557/APJCP.2022.23.10.3507

Meulmeester E, Ten Dijke P (2011): The dynamic roles of TGF-β in cancer. J. Pathol. **223,** 205-218 https://doi.org/10.1002/path.2785

Mei L, Zhang Z (2021): Advances in biological application of and research on low-frequency ultrasound. Ultrasound Med. Biol. **47,** 2839-2852 https://doi.org/10.1016/j.ultrasmedbio.2021.06.005

Qian L, Thapa B, Hong J, Zhang Y, Zhu M, Chu M, Yao J, Xu D (2018): The present and future role of ultrasound targeted microbubble destruction in preclinical studies of cardiac gene therapy. J. Thorac. Dis. **10,** 1099-1111 https://doi.org/10.21037/jtd.2018.01.101

Schmid RS, Maness PF (2008): L1 and NCAM adhesion molecules as signaling coreceptors in neuronal migration and process outgrowth. Curr. Opin. Neurobiol. **18,** 245-250 https://doi.org/10.1016/j.conb.2008.07.015

Seoane J, Le HV, Shen L, Anderson SA , Massagué J (2004): Integration of Smad and forkhead pathways in the control of neuroepithelial and glioblastoma cell proliferation. Cell **117,** 211-223 https://doi.org/10.1016/S0092-8674(04)00298-3

Sun WL, Kang T, Wang YY, Sun JP, Li C, Liu HJ, Yang Y, Jiao BH (2019): Long noncoding RNA OIP5-AS1 targets Wnt-7b to affect glioma progression via modulation of miR-410. Brain Res. **39,** BSR20180395 https://doi.org/10.1042/BSR20180395

Wang LY, Zheng SS (2019): Advances in low-frequency ultrasound combined with microbubbles in targeted tumor therapy. J. Zhejiang. Univ. Sci. B. **20,** 291-299 https://doi.org/10.1631/jzus.B1800508

Wei KC, Chu PC, Wang HY, Huang CY, Chen PY, Tsai HC, Lu YJ, Lee PY, Tseng IC, Feng LY, et al. (2013): Focused ultrasound-induced blood-brain barrier opening to enhance temozolomide delivery for glioblastoma treatment: a preclinical study. PloS One **8,** e58995 https://doi.org/10.1371/journal.pone.0058995

Wesolowska A, Kwiatkowska A, Slomnicki L, Dembinski M, Master A, Sliwa M, Franciszkiewicz K, Chouaib S, Kaminska B (2008): Microglia-derived TGF-beta as an important regulator of glioblastoma invasion--an inhibition of TGF-beta-dependent effects by shRNA against human TGF-beta type II receptor. Oncogene **27,** 918-930 https://doi.org/10.1038/sj.onc.1210683

Willems E, Cabral-Teixeira J, Schade D, Cai W, Reeves P, Bushway PJ, Lanier M, Walsh C, Kirchhausen T, Izpisua Belmonte JC, Cashman J, et al. (2012): Small molecule-mediated TGF-β type II receptor degradation promotes cardiomyogenesis in embryonic stem cells. Cell Stem Cell **11,** 242-252 https://doi.org/10.1016/j.stem.2012.04.025

Yao L, Zhang Z (2019): The reversal of MRP1 expression induced by low-frequency and low-intensity ultrasound and curcumin mediated by VEGF in brain glioma. OncoTargets Ther. **12,** 3581-3593 https://doi.org/10.2147/OTT.S195205

Zhang L, Yin T, Li B, Zheng R, Qiu C, Lam KS, Zhang Q, Shuai X (2018): Size-modulable nanoprobe for high-performance ultrasound imaging and drug delivery against cancer. ACS Nano. **12,** 3449-3460 https://doi.org/10.1021/acsnano.8b00076

Zhang W, Shen Q, Peng ZY (2011): Establishment of NCAM L1 minigene model and its splicing patterns in different cell lines. J. Zhejiang Univ. **40,** 427

Zhang Z, Chen J, Chen L, Yang X, Zhong H, Qi X, Bi Y, Xu K (2012): Low frequency and intensity ultrasound induces apoptosis of brain glioma in rats mediated by caspase-3, Bcl-2, and survivin. Brain Res. **1473,** 25-34 https://doi.org/10.1016/j.brainres.2012.06.047

Zhang Z, Xu K, Bi Y, Yu G, Wang S, Qi X, Zhong H (2013): Low intensity ultrasound promotes the sensitivity of rat brain glioma to Doxorubicin by down-regulating the expressions of p-glucoprotein and multidrug resistance protein 1 in vitro and in vivo. PloS One **8,** e70685 https://doi.org/10.1371/journal.pone.0070685

Zhao B, Chen Y, Liu J, Zhang L, Wang J, Yang Y, Lv Q, Xie M (2017): Blood-brain barrier disruption induced by diagnostic ultrasound combined with microbubbles in mice. Oncotarget **9,** 4897-4914 https://doi.org/10.18632/oncotarget.23527

Zhao R, Liang X, Zhao B, Chen M, Liu R, Sun S, Yue X, Wang S (2018): Ultrasound assisted gene and photodynamic synergistic therapy with multifunctional FOXA1-siRNA loaded porphyrin microbubbles for enhancing therapeutic efficacy for breast cancer. Biomaterials **173,** 58-70 https://doi.org/10.1016/j.biomaterials.2018.04.054

Zhu C, Fang Z, Peng L, Gao F, Peng W, Song F (2022): Curcumin suppresses the progression of colorectal cancer by improving immunogenic cell death caused by irinotecan. Chemotherapy **67,** 211-222 https://doi.org/10.1159/000518121

Received: January 21, 2023
Final version accepted: July 19, 2023